Available at https://www.iasj.net/iasj
Iraqi Academic Scientific Journals
Journal homepage:
https://journals.uokerbala.edu.iq/index.php/UOKJ

Research Article

Determining the Optimal Values for Certain Rate Equation Parameters of the Cr: LiSAF Laser with Cr: YSO as a Saturable Absorber Through an Optimization Technique

[1,]Duaa Sabbar Salman [2,] Qasim Hassan Ubaid

[1,2,]University of Kerbala ,College of Science,Department of physics

Article Info
Article history:
Received 15 -5-2025
Received in revised form 1-6-2025
Accepted 16-6-2025
Available online 30 -6 -2025
Keywords:
Q-switching laser, Cr: LiSAF, Cr: YSO, optimization.

Abstract:

Q-switching is a technique employed for control a laser system, enabling the generation of brief, high-energies laser pulses. The purpose of this study is to identify optimal values for certain rate equation parameters using an optimization technique. The Runge – Kutta – Fehlberg approach was employed to simulate the rate equations to find pulse characteristics of a Cr: LiSAF laser with Cr: YSO as a saturable absorber under a certain condition. The Rosenbrock optimization technique was used to find the optimal values of the decision variables (β, γa, γc) for different saturable absorber molecules number. The values of γa and γc are found to decrease with the increasing number of molecules due to the decrease in the absorption of photons by the material as a result of reaching the saturation state. For the β parameter, the increase in the saturable absorber molecules number leads to an increase in its value. According to the computer code, the calculated energy value was 4.19 mJ compared to the published 4.3 mJ, while the pulse duration is 35.1 nsec compared with 35 nsec.

Corresponding Author E-mail : duaa.s@s.uokerbala.edu.iq , Qasim.hassan@uokerbala.iq
Peer review under responsibility of Iraqi Academic Scientific Journal and University of Kerbala.

1. INTRODUCTION

A Q-switched laser is a kind of a pulsed laser that reduces pulse duration, enhances peak output power, and increases output consistency between pulses[1-5]. These pulses can be generated using several approaches, including cavity dumping, and both active and passive Q-switching. This work used passive Q-switching technology, because of the advantages of this technology from simple construction, compact size, low cost, enhanced durability and dependability, and does not need intricate additional cavity modulation devices. It generates brief pulses and elevated peak powers[6, 7]. This technique produces large pulses[8]. the pumping process facilitates the establishment of a population inversion and gain within the active medium, exceeding typical levels observed during free-running operation, without inducing oscillations, as demonstrated in Fig.1[9, 10].

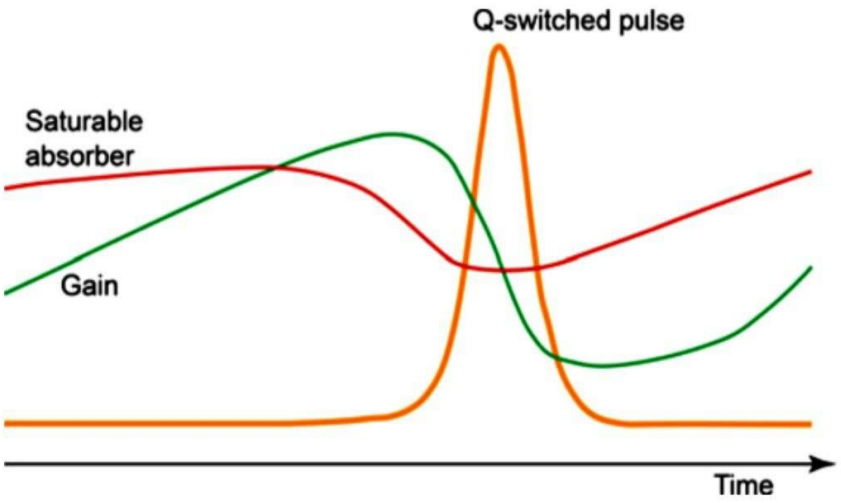

Fig. 1.: Dynamics of a passively Q-switched laser [9].

This technique on contingent upon the saturable absorber material, which exhibits pronounced nonlinear absorption characteristics, influenced by the material's lifetime, absorption cross-section, energy levels, and the molecular number density within these levels, in comparison to other materials. It exhibits significant absorption at low intensity of light and can be somewhat bleached depending on its absorption capacity when the light intensity increases[11]. This technology has several practical applications, including medical science[12], precise measurement[13], spectral analysis[14], and distance finders[13, 15]. Over past four decades, there has been significant interest in a new mathematical discipline called "optimization." Optimization strategies focus on identifying the optimal solution while considering both cost-effectiveness and safety[16-18]. In particular, recent years have seen significant focus on enhancing the efficacy of Q-switched lasers[19]. Generally, there are two methodologies for optimizing passively Q-switched lasers. The initial method examines the rate equations governing the Q-switched laser, yielding a fundamental analysis relationship for the selected input parameters and the maximum pulse energy, as well as the minimum pulse width. The second technique involves the production of a set of graphically charts that illustrate the laser output properties.

2. MATERIALS

In this work, a Cr: LiSAF laser of wavelength 880 nm was used as an active medium with Cr: YSO as a saturable absorber. This choice was based on the compatibility of the laser emission spectrum with the absorption spectrum of the saturable absorber, as well as the characteristics of the laser and the saturable absorber.

The Cr:LiSAF solid-state laser was initially identified in 1989[20], its extensively adjustable from 780 nm to 920 nm and has garnered interest during the last decade[21, 22]. The greatest wavelength of the free-running laser beam is around 850 nm[23, 24]. Numerous robust solid-state saturable absorbers are documented to functioning well at solid-state lasers across diverse wavelengths[7, 25, 26]. Tunable Q-switched solid-state lasers are particularly noteworthy among passively Q-switched solid-state lasers, since they enable the adjustment of the laser wavelength to meet specific requirements. Experimental evidence demonstrates that the Cr: YSO saturable absorber can efficiently Q-switch the Cr: LiSrAlF6 (Cr: LiSAF) laser at wavelength in 880 nm. It can also serve as a Q-switch for many lasers such as: Cr: LiCAF, alexandrite, and ruby lasers[27]. In 1961, Warshaw et al. produced Cr: YSO via a chemical technique. It a purely tetravalent chromium system[28]. Among of its significant material characteristics are: Owns a refractive index of 1.8 , a damage threshold of up to 30 J/cm², a melting point of 2070 C^0 [29, 30]. It exhibits four absorption bands with peaks at around 390 nm, 595 nm, 695 nm, and 750 nm, as seen in Fig. 2.

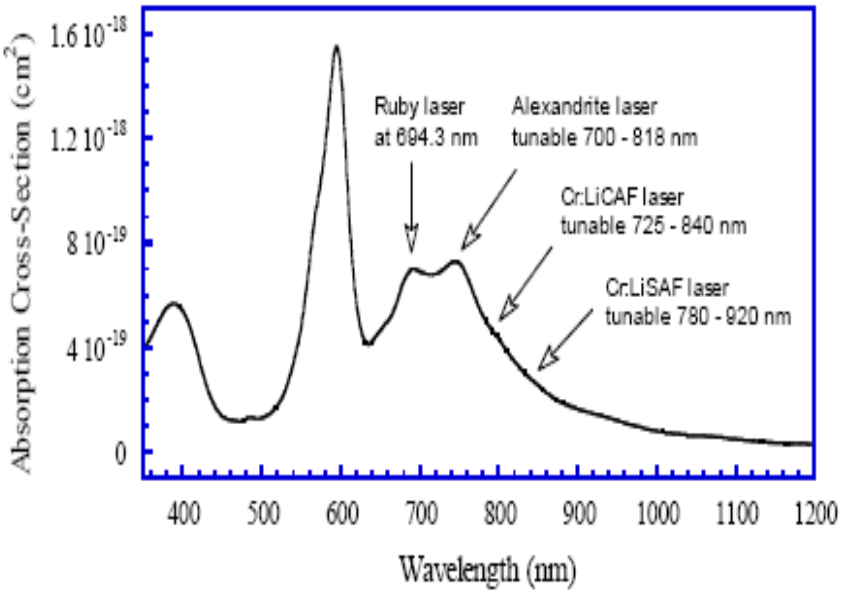

Fig. 2.: Cr 4+:Y2SiO5 absorption spectrum[29]

There are several applications for this material with Cr: LiSAF lasers, including remote sensing, precision cutting, marking materials, and in medicine to treat skin diseases [27, 31, 32]

3. METHODS

3.1. NUMERICAL SIMULATION

Szabo & Stein in 1965[33] proposed a system of rate equations based on a two-energy-level model. YK Kuo, MF Huang& M Birnbaum in 1995[34] expanded this model to include three energy levels. The three coupled-rate equations in reference[35] have been revised to form a model of four coupled-rate equations. We used the Runge – Kutta – Fehlberg approach for numerically solving the rate equations, through simulation by a computer program we wrote to describe the behavior of the system.

$$\frac{dn}{dt}=[K_g N_g - K_a N_a - \beta K_a N_{au} - \gamma_c]n \quad (1)$$

$$\frac{dN_g}{dt}=R_p - \gamma_g N_g - K_g N_g n \quad (2)$$

$$\frac{dN_a}{dt}=\gamma_a N_{au} - K_a N_a n \quad (3)$$

$$\frac{dN_{au}}{dt}=K_a N_a n - \gamma_a N_{au} \quad (4)$$

n is the photon number inside the laser resonator.

N_g is the population inversion of active medium.

K_g is the coupling coefficient between the stimulated photons and the active medium element.

N_a is the ground state population of the saturable absorber.

N_{au} is the first excited state population of the saturable absorber.

R_p is the pumping rate (sec^{-1}).

K_a is a coupling coefficient between photons and the saturable absorber molecules.

γ_a is the saturable absorber decay rate(sec^{-1}).

γ_g= 1/τg is the effective decay rate of the upper laser level(sec^{-1})[36].

The first equation denotes the rate equation for the cavity photon number (n).

The second equation denotes the rate equation for the gain medium (N_g)

The third equation denotes the rate equation for saturable absorber molecule at the ground state (N_a).

The fourth equation represents the rate equation for saturable absorber molecules at the first excited state (N_{au})[37].

We provided the program with the following inputs taken from experimental references[27, 38]:

$\gamma_g = 1.49\times10^{4}\ s^{-1}$, $K_g = 4.03\times10^{-9}\ s^{-1}$, $K_a = 1.52\times10^{-8}\ s^{-1}$, and $N_{a0} = 2.30\times10^{16}$

3.2. OPTIMIZATION TECHNIQUE

The constrained Rosenbrock optimization technique was used to find the optimum values of the decision variables ($\beta, \gamma_a, \gamma_c$). The reason behind choosing this technique is that it meets all the requirements of our problem, which has the following characteristics: Non-linear, multivariable, and constrained. The constrained Rosenbrock approach is categorized as a numerical multivariable search methodology that addresses confined variables in a nonlinear context[39, 40]. The algorithm proceeds per unconstrained Rosenbrock procedure until convergence is reached or a boundary zone near the constrained is entered. It depends on rotating the axes and repetition to find the optimal values[41], as the number of repetitions in our study ranged between 1000- 3000 times. The stopping condition for the program was set so that the difference between the penalty function (Equation 4) and the number of input molecules was less than 10^{-3}.

We linked the optimization program with the simulation program, so they became one code. The optimal values of the decision variables ($\beta, \gamma_a, \gamma_c$) were found using this technique. The ground state population of the saturable absorber (N_a) must exceed the population of the first excited state (N_{au}) during the rising time $N_{au} < N_a$, (β)value between 0.2 to 0.9 Because the absorption cross section of the first excited state is less than the absorption cross section of the ground state, its value is always less than 1, (γ_a)value between 1E+6 to 7E+6 this parameter indicates the speed of the transfer of molecules from higher levels to lower levels. It is a non-radiative transfer and depends on the speed of the material's response in absorbing the light falling on it. Its value is low because the energy levels are close to each other. It is the reciprocal of the relaxation time of the saturable absorber material [42, 43],

(γ_c)value between 1E+08 to 7E+08 this parameter refers to the total photons losses within the resonator, which include diffraction, absorption, refraction, and reflection, which have a direct effect on the laser intensity. The higher the loss, the lower the laser intensity. The photon losses must be less than the gain in order for the laser to be achieved [42]. In this study, the range (γ_a, γ_c)was extended so that the algorithm search is within a wide range, which makes the solution more flexible. On (β,γ_a,γ_c) were dealt with by step size of (0.001,0.1,1) respectively. The pulse energy and duration under this optimal condition were found to be 4.19 mJ and 35.1 nsec, respectively. Relative error between the calculated and published in reference[38] of the pulse energy and duration were 0.02, 0.002 respectively, which confirms the validity of the obtained results.

4. RESULTS & DISCUSSION

4.1. FINDING THE OPTIMUM VALUES FOR SOME RATE EQUATIONS PARAMETERS

The maximization option for the objective functions (the rate equations in our case) was used to get the values of β, γ_a,γ_c as shown in table (1).

Table 1. Optimum values of β, γa, γc at different molecules numbers.

Molecule Numbers x 10^{16}	Optimum β values	Optimum γ_a values Sec $^{-1}$	Optimum γ_c values Sec $^{-1}$	Pulse Duration nsec	Pulse Energy mJ	Pulse power Watt
2.3	0.3001	1430009	129000320	35.1	4.19	119429.35
3.3	0.3002	1349229	129000321	19.39	8.36	431236.91
4.3	0.3005	1429994	129000456	16.41	14.74	898024.86
5.3	0.3382	1200081	129559971	15.77	25.34	1637520.66
6.3	0.3580	1200083	127782046	12.46	25.11	2014763.57
7.3	0.4084	1200020	124607628	9.76	48.76	4993090.63

Fig. 3 shows the pulse of a Cr: LiSAF laser with Cr: YSO as a saturable absorber, which depends mainly on the number of saturable absorber molecules, the number of levels participating in absorption, and the absorption cross-sectional area. We noticed by performing the optimization for (β) that increasing the absorption cross-section results in an augmentation of the pulse energy. The reason for this could be explained by increasing the absorption cross-section, the absorption activity of the saturable absorbent material increases, which in turn leads to a high energy storage in the laser medium. As demonstrated in the following fig. 4.

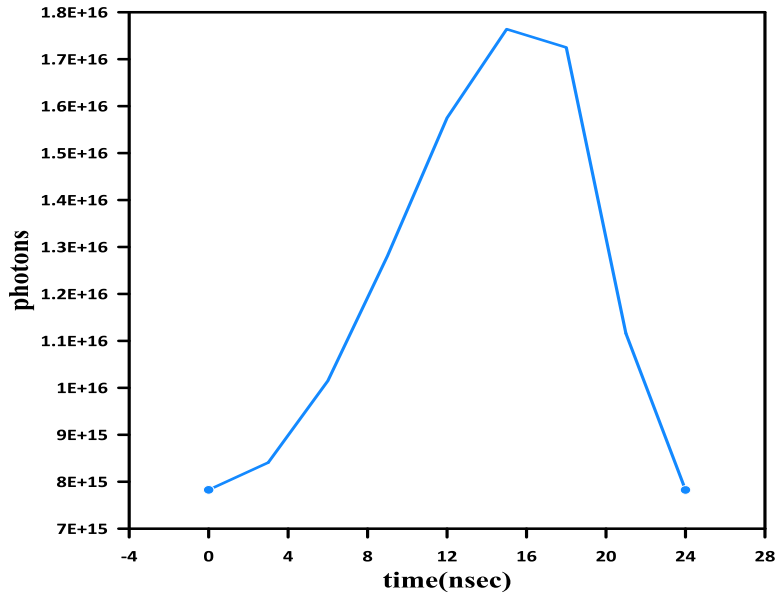

Fig.3. Stimulated photon cavity profile while using 2.3 $\times 10^{16}$ molecules for the saturable absorber molecules number.

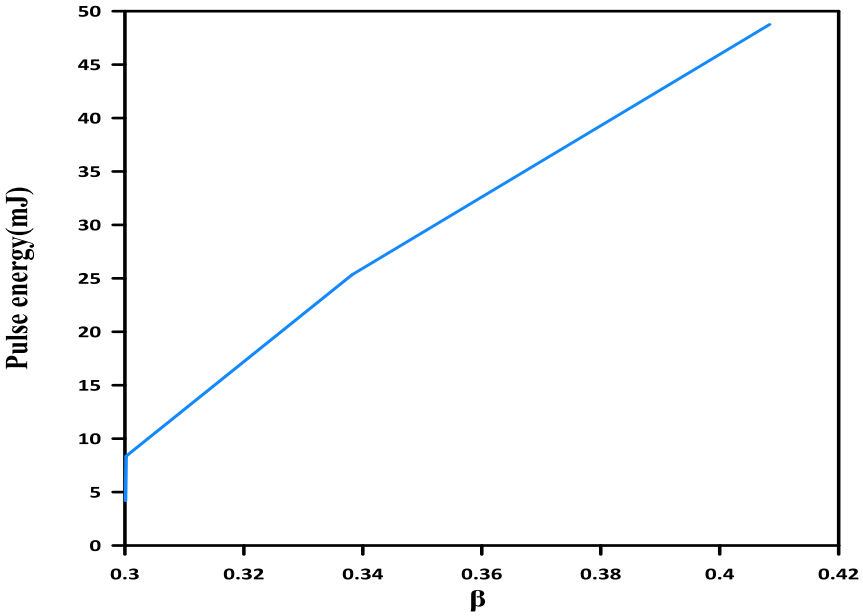

Fig.4.: The β parameter as a function of pulse energy. The amount of energy increases with increasing value of β due to the increase in the absorption capacity of the saturable absorber material.

4.2. OPTIMUM VALUES OF RELAXATION RATE SATURABLE ABSORBER AT DIFFERENT VALURE OF MOLECULES NUMBER OF SATURABLE ABSORBER(γ_a)

We noticed from the results obtained during our study that increasing the number of saturable absorber molecules material from 2.3× 10^{16} to 7.3× 10^{16}, leads to a decrease in the relaxation rate of the saturable absorbent until reaching a certain limit where the change is not

clear and it can be considered constant due to the material reaching the saturation state. The transfer of saturable absorber molecules from the fundamental state to the upper state is negligible. This is due the quantity of molecules in each energy level is determined by the Boltzmann distribution (The Boltzmann distribution governs the population of energy states in a solid. It predicts that particles favor low-energy states, and the occupation probability of higher-energy states decreases exponentially with energy, according to the following relationship: $N_i = \frac{N}{Z}\, g_i e^{-E_i/K_B T}$, N_i is the average number of particles in the set of states with energy E_i, N is the total number of molecules, N is the degeneracy of energy level i, Z is the partition function, E_i is the energy of the i-th energy level, K_B is the Boltzmann constant, T is absolute temperature [44]).The increase of Cr: YSO molecules in the ground state will lead to a little increase in the number of molecules in the first excited state. Therefore, this will not improve the intersystem crossing rate. Finally, this parameter leads to an augmentation of the material's relaxation time and the pulse energy. As shown in the following fig. 5,6,7.

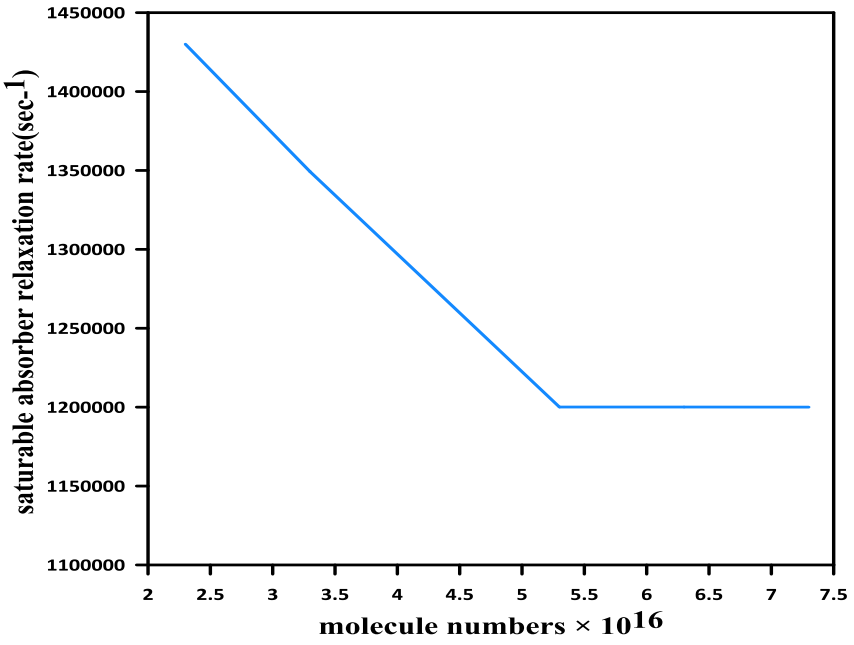

Fig. 5. The profile of relaxation rate as a function of Cr: YSO molecule numbers. The relaxation rate values decrease as the number of saturable absorber molecules increases until reach a certain value is reached, where the variation becomes insignificant.

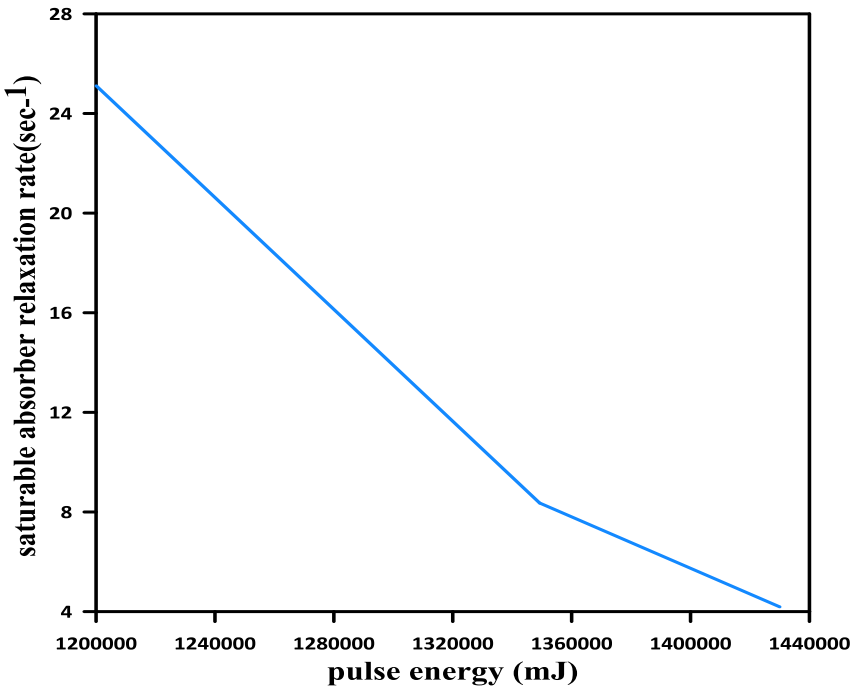

Fig. 6. Relaxation rate as a function of pulse energy. Increase in pulse energy with decrease in Relaxation rate of saturable absorbent material due to the material reaching saturation state.

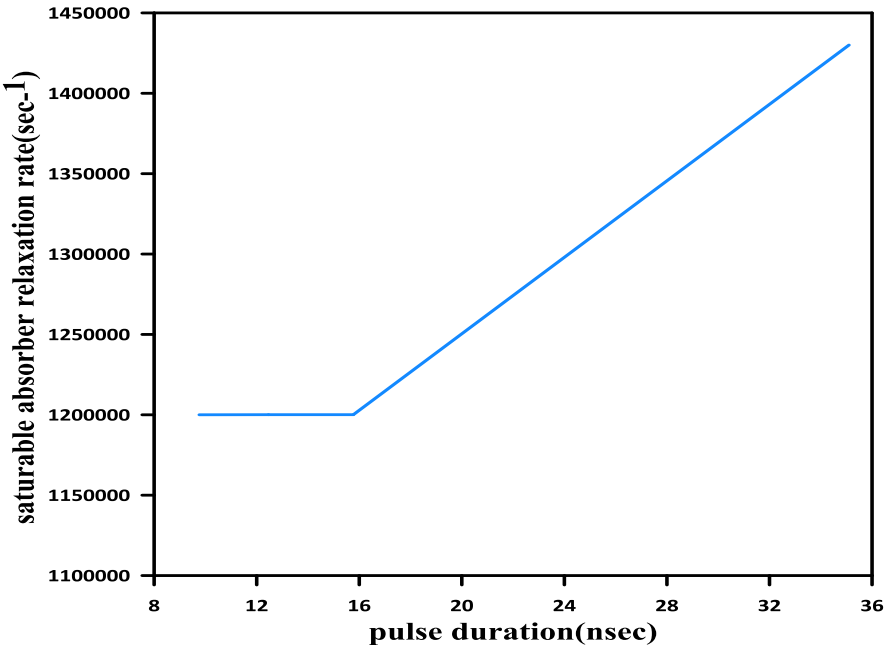

Fig. 7. Relaxation rate as a function of pulse duration. The increase in pulse energy due to the decrease in Relaxation rate resulted in a decrease in pulse duration.

4.3. OPTIMUM VALUES OF DECAY RATE AT DIFFERENT VALUES OF MOLECULES AVERAGE CAVITY PHOTON NUMBER OF SATURABLE ABSORBER (γ_c)

When photons leave the active medium, they fall on the saturable absorber material then it is absorbed by the fundamental state molecules. These molecules are elevated to the initial excited state. This causes high photon losses inside the resonator and provides high inverse population in the active medium (high energy storage) as a result of preventing stimulated emission from happening. This absorption continues until the material reaches the saturation state; the vast majority of molecules move to the upper levels. At this moment, photon losses begin to decrease, the material becomes transparent, and a pulse of high energy and short duration is emitted, as shown in the fig. 8,9,10.

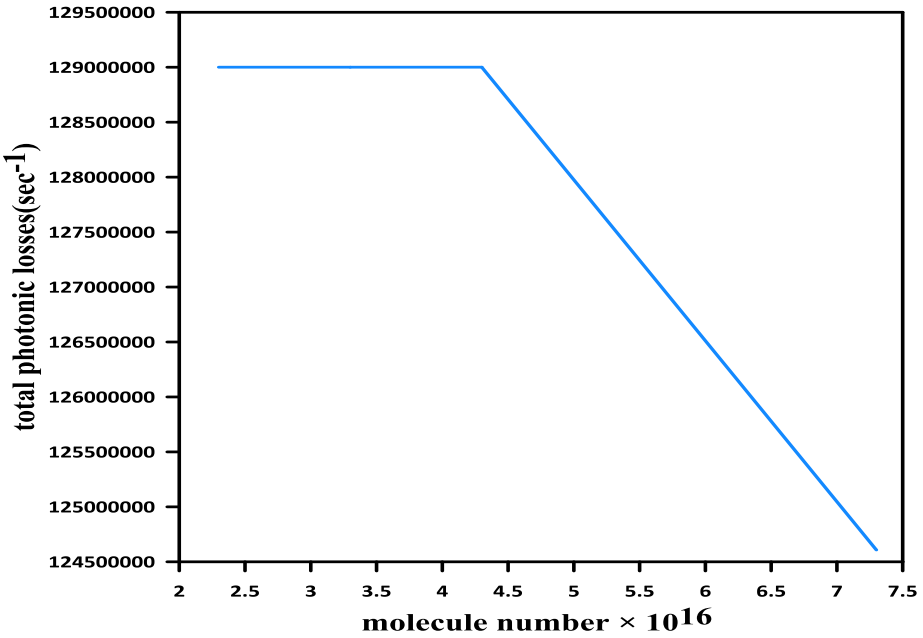

Fig. 8. The profile of total photonic losses as a function of Cr: YSO molecules number. The value of total photonic losses decreases with increasing number of molecules because the maximum absorption of the saturable absorber is at the initial value of molecules.

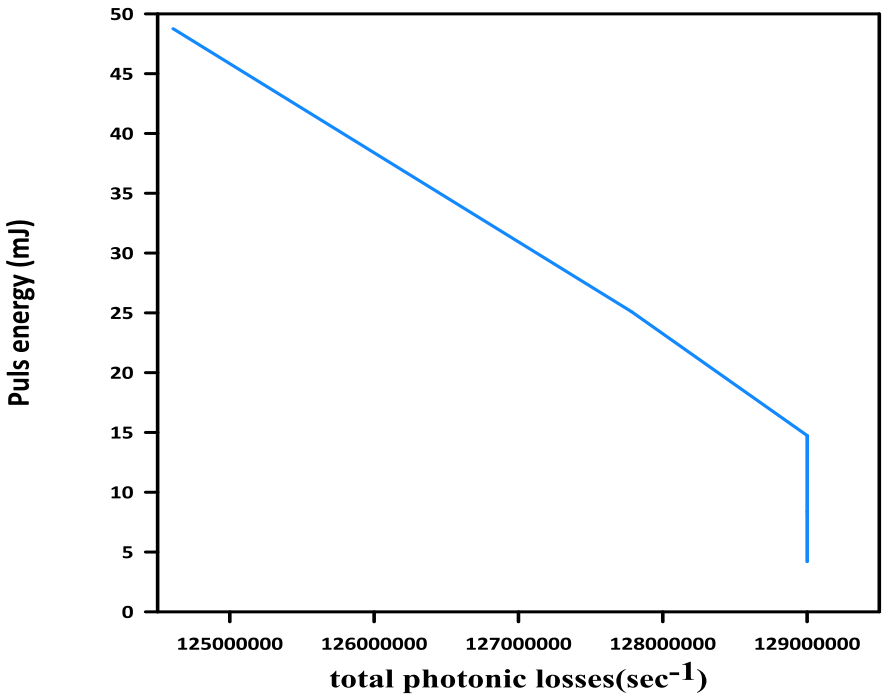

Fig. 9. Total photonic as a function of pulse energy. Increasing the value of the inverse population of the active medium leads to an increase in the pulse energy.

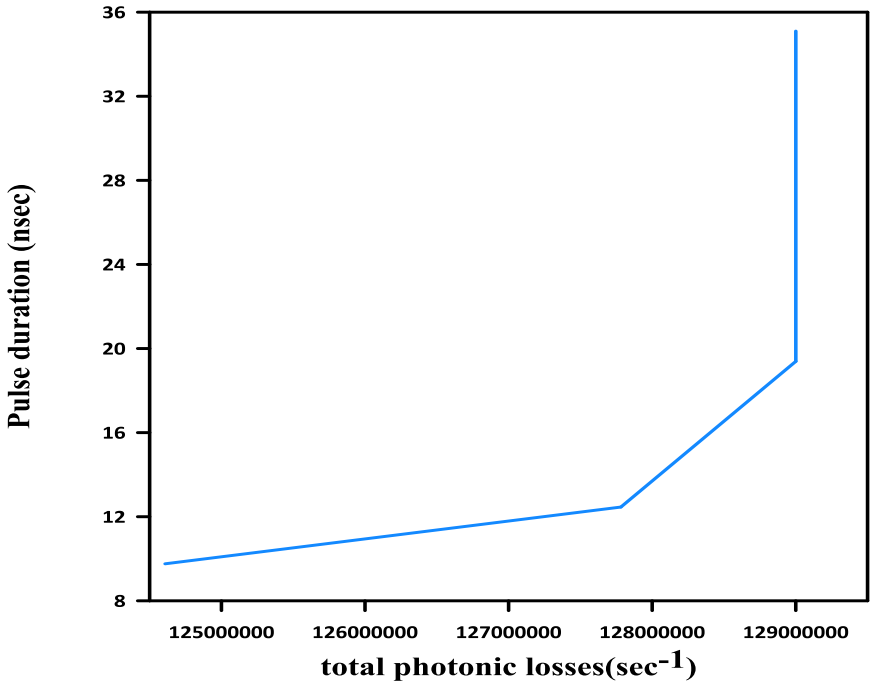

Fig. 10. Total photonic as a function of pulse duration.

5. CONCLUSIONS

A Cr: LiSAF laser pulse simulated with Cr: YSO as a saturable absorber by solving the rate equations using a computer program. Then, the constrained Rosenbrock optimization method was used to find the optimal values of $(\beta, \gamma_a, \gamma_c)$. This technique proved effective in finding the optimum values of the decision variables. We concluded that the value of γ_a, γ_c decreases with the increase in the number of molecules, but β increases, the growth will continue until a specific value is reached, after which the increment in the saturable absorber molecules number will by a non-influential amount.

6. REFERENCE

1. Kurkov, A. (2011). Q-switched all-fiber lasers with saturable absorbers. *Laser Physics Letters, 8*(5), 335–342.
2. Shen, Y., Fu, X., Yao, C., Li, W., Wang, Y., Zhao, X., … & Ning, Y. (2022). Optical crystals for 1.3 μm all-solid-state passively Q-switched laser. *Crystals*, *12*(8), 1060.
3. Popa, D., Sun, Z., Hasan, T., Torrisi, F., Wang, F., & Ferrari, A. C. (2011). Graphene Q-switched, tunable fiber laser. *Applied Physics Letters*, *98*(7).
4. Tang, Y., & Xu, J. (2015). A random Q-switched fiber laser. *Scientific Reports*, *5*, 9338.
5. Skorczakowski, M., Swiderski, J., Pichola, W., Nyga, P., Zajac, A., Maciejewska, M., ... & Bragagna, T. (2010). Mid-infrared Q-switched Er: YAG laser for medical applications. *Laser physics letters*, *7*(7), 498.
6. Pérez-Alonso, V., Weigand, R., Sánchez-Balmaseda, M., & Pérez, J. G. (2023). Powerful algebraic model to design Q-switched lasers using saturable absorbers. *Optics & Laser Technology*, *164*, 109506.
7. Zhang, X., Zhong, K., Qiao, H., Li, F., Zheng, Y., Xu, D., & Yao, J. (2021). Passively Q-switched dual-wavelength laser operation with coaxially end-pumped composite laser materials. *IEEE Photonics Journal*, *13*(6), 1–7.
8. Li, L., Cheng, J., Zhao, Q., Zhang, J., Yang, H., Zhang, Y., … & Liu, W. (2023). Chromium oxide film for Q-switched and mode-locked pulse generation. *Optics Express*, *31*(10), 16872–16881.
9. Keller, U., & Paschotta, R. (2021). *Ultrafast lasers*. Springer.
10. Perrière, C., Boulesteix, R., Maitre, A., Forestier, B., Jalocha, A., & Brenier, A. (2021). Study of dopant distribution in Cr4+: YAG transparent ceramics and its use as passively Q-switching media in Nd: YAG laser delivering 38 mJ per pulse. *Optical Materials: X*, *12*, 100107.
11. Ismail, M. A., Harun, S. W., Ahmad, H., & Paul, M. C. (2016). Passive Q-switched and mode-locked fiber lasers using carbon-based saturable absorbers. In *Fiber Laser*. IntechOpen.
12. Wang, J., Xie, L., Wang, Y., Lan, Y., Wu, P., Lv, J., ... & Cheng, G. (2023). High-damage vanadium pentoxide film saturable absorber for sub-nanosecond Nd: YAG lasers. *Infrared Physics & Technology*, *129*, 104580.
13. Li, M., Qin, Y., Wang, C., Liu, X., Long, S., Tang, X., & Wen, T. (2019). Nonuniform pumped passively Q-switched laser using Nd: YAG/Cr4+: YAG composite crystal with high-pulse energy. Optical Engineering, 58(3), 036106-036106.
14. Zhao, Z. Y., Cai, Z. T., Zhao, C. M., & Zhang, J. (2023). Solar-pumped 1061-/1064-nm dual-wavelength Nd: YAG monolithic laser. *Optical Engineering*, *62*(3), 036103-036103.

15. Ali, Z., Abdulsada, Z., Arasavalli, N., Kadhim, S., & Akram, H. (2023). Initial Transmission Influence on Saturable Absorber Absorption Activity of Passive Q-Switching Erbium-Doped Fiber Laser System. *University of Thi-Qar Journal of Science*, *10*(2), 224-229.
16. Diwekar, U. M. (2020). *Introduction to applied optimization* (Vol. 22). Springer Nature.
17. Crown, W., Buyukkaramikli, N., Thokala, P., Morton, A., Sir, M. Y., Marshall, D. A., … & Pasupathy, K. S. M. Baudin. (2011). *Introduction to unconstrained optimization*.
18. Baudin, M. (2011). Introduction to Unconstrained Optimization.
19. Patel, F. D., & Beach, R. J. (2001). New formalism for the analysis of passively Q-switched laser systems. *IEEE Journal of Quantum Electronics*, *37*(5), 707–715.
20. Payne, S. A., Chase, L. L., Smith, L. K., Kway, W. L., & Newkirk, H. W. (1989). Laser performance of LiSrAlF6: Cr3+. *Journal of Applied Physics*, *66*(3), 1051-1056.
21. Beaud, P. A., Richardson, M., & Miesak, E. J. (1995). Multi-terawatt femtosecond Cr:LiSAF laser. *IEEE Journal of Quantum Electronics*, *31*(2), 317–325.
22. Dymott, M., & Ferguson, A. (1994). Self-mode-locked diode-pumped Cr:LiSAF laser. *Optics Letters*, *19*(23), 1988–1990.
23. Koechner, W. (2013). *Solid-state laser engineering* (Vol. 1). Springer.
24. Stalder, M., Chai, B. H., & Bass, M. (1991). Flashlamp pumped Cr-LiSrAlF6 laser. *Applied Physics Letters*, *58*(3), 216.
25. Zhang, D., Su, L., Li, H., Qian, X., & Xu, J. (2006). Characteristics and optical spectra of V:YAG crystal grown in reducing atmosphere. *Journal of Crystal Growth*, *294*(2), 437–441.
26. Hassan, A. A., Wahid, S. N. A., & Hamood, H. Y. (2021). Numerical modeling of passively Q-switched Nd:YAG lasers with Cr:YAG as a saturable absorber.
27. Chen, H.-F., Hsieh, S.-W., & Kuo, Y.-K. (2005). Simulation of tunable Cr:YSO Q-switched Cr:LiSAF laser. In *High-Power Lasers and Applications III*. SPIE.
28. Kuo, Y.-K., Chen, H.-M., & Chang, J.-Y. (2001). Numerical study of the Cr:YSO Q-switched ruby laser. *Optical Engineering*, *40*(9), 2031–2035.
29. Kuo, Y.-K., Chang, J., & Chen, H. (2000). Broadband Cr:YSO solid-state saturable absorber for ruby, alexandrite, and Cr:LiCAF lasers: Numerical study on passive Q-switching performance. In *Optoelectronic Materials and Devices II*. SPIE.
30. Kuo, Y.-K., & Chen, H.-M. (2000). Tunable Cr:YSO Q-switched Cr:$BeAl_2$ O_4 laser: Numerical study on laser performance along three principal axes of the Q switch. *Japanese Journal of Applied Physics*, *39*(7R), 4002.
31. Van Hao, N., Minh, P. H., Van Duong, P., & Dai Hung, N. (2014). Numerical investigations of laser diode end-pumped solid-state Cr^{3+}:LiSAF lasers passively Q-switched with Cr^{4+}:YSO crystal. *Communications in Physics*, *24*(3S2), 71–84.
32. Mekteplioglu, M. F., Ozturk, Y., Kärtner, F. X., & Demirbas, U. Q-switched mode-locked Cr: LiSAF laser with broad tunability.
33. Szabo, A., & Stein, R. (1965). Theory of laser giant pulsing by a saturable absorber. *Journal of Applied Physics*, *36*(5), 1562–1566.
34. Kuo, Y.-K., Huang, M.-F., & Birnbaum, M. (1995). Tunable Cr^{4+}:YSO Q-switched Cr:LiCAF

laser. *IEEE Journal of Quantum Electronics, 31*(4), 657–663.
35. Chang, C.-K., Chang, J., & Kuo, Y.-K. (2002). Optical performance of Cr:YSO Q-switched Cr:LiCAF and Cr:LiSAF lasers. In *High-Power Lasers and Applications II*. SPIE.
36. Kalashnikov, V. L., Shcherbitsky, V. G., Kuleshov, N. V., Girard, S., & Moncorge, R. (2002). Pulse energy optimization of passively Q-switched flash-lamp pumped Er:glass laser. *Applied Physics B, 75*, 35–39.
37. Salih, A.-K. M. (2014). Influence of absorption cross section of saturable absorber on passive Q-switching laser pulse characteristics. *University of Thi-Qar Journal of Science*, *4*(4), 99–104.
38. Munin, E., Villaverde, A. B., Zhang, X. X., & Bass, M. (1993). Broad-band, intensity-dependent absorption in tetravalent chromium-doped crystals. *Applied Physics Letters*, *63*(13), 1739.
39. Ma, J., & Li, H. (2019). Research on Rosenbrock function optimization problem based on improved differential evolution algorithm. *Journal of Computer Communications*, *7*(11), 107–120.
40. Benner, P., & Mena, H. (2013). Rosenbrock methods for solving Riccati differential equations. *IEEE Transactions on Automatic Control*, *58*(11), 2950–2956.
41. Mize, J. P. (1973). *Optimization techniques with FORTRAN*. McGraw-Hill, Inc.
42. Kuo, Y.-K., Chen, H.-M., & Lin, C.-C. (2000). A theoretical study of the Cr: $BeAl_2O_4$ laser passively Q-switched with Cr: YSO solid state saturable absorber. *Chinese Journal of Physics*, *38*(3), 443–460.
43. Azzouz, I. M., & El-Nozahy, A. (2006). Numerical study of Cr^{4+}:YAG passively Q-switching Nd:$GdVO_4$ laser. *Egyptian Journal of Solids*, *29*(1), 215–225.
44. Atkins, P. W., De Paula, J., & Keeler, J. (2023). *Atkins' Physical Chemistry*. Oxford University Press.